Available online at www.sciencedirect.com
SCIENCE DIRECT
Tetrahedron
Tetrahedron 62 (2006) 3065–3074

Construction of divergent anthracene arrays within dendritic frameworks

Masaki Takahashi,[a,*] Hironao Morimoto,[b] Yousuke Suzuki,[a] Mitsuji Yamashita,[a] Hideki Kawai,[c] Yoshihisa Sei[d] and Kentaro Yamaguchi[d]

[a]*Department of Materials Science and Chemical Engineering, Faculty of Engineering, Shizuoka University, 3-5-1 Johoku, Hamamatsu, Shizuoka 432-8561, Japan*
[b]*Graduate School of Science and Engineering, Shizuoka University, 3-5-1 Johoku, Hamamatsu, Shizuoka 432-8561, Japan*
[c]*Research Institute of Electronics, Shizuoka University, 3-5-1 Johoku, Hamamatsu, Shizuoka 432-8011, Japan*
[d]*Faculty of Pharmaceutical Sciences at Kagawa Campus, Tokushima Bunri University, Shido, Sanuki, Kagawa 769-2193, Japan*

Received 5 December 2005; revised 6 January 2006; accepted 10 January 2006

Available online 30 January 2006

Abstract—This publication presents simple methodologies for construction of divergent anthracene arrays either within structural interior or at peripheral positions of dendritic frameworks. The synthetic approaches employed multiple coupling reactions between two types of 10-functionalized 9-anthryl chlorides and two types of polyphenolic linkers, resulting in four types of dendritic architectures. Successful implementation of the syntheses was confirmed by a range of spectroscopies along with elemental analyses and size exclusion chromatography studies. The resulting dendritic molecules showed a range of solubilities in chloroform fairly affected by the dendritic backbone structures. Fluorescence spectroscopic experiments of the multichromophoric dendritic systems indicated pronounced energy delocalization functionalities via an energy migration within the branched molecular frameworks as expressed in reduced fluorescence quantum yields and complex emission decay profiles.

1. Introduction

Over the last decade, there has been a rapid increase in the literature published on new dendritic architectures because of their potential applications in the new emerging field of nanotechnology.[1,2] The dendritic frameworks provide unique nanometer-size environments, which may serve as a polymer backbone for effective three-dimensional matrices due to their highly branched and compressed globular structures.[3,4] In this context, functional elements embedded within the dendritic skeletal frameworks may define shell effects of the dendritic architectures, which render the resulting hyperbranched systems potentially versatile. Nevertheless, a major focus of contemporary synthetic approaches to dendrimers is functionalization of surface groups and structural modification of core units because most of the functionalized molecular materials are synthetically dormant due to their structural complexity, which may result in poor feasibility to be incorporated into the dendritic systems.[5] In previous publications, we have reported that first-generation architectures such as *n*-hexyl substituted dendron **1** and dendrimer **2** (Fig. 1) showed cooperative action of the chromophoric groups leading to energy delocalization of absorbed photons.[6,7] It has been recognized in this context that such chromophore-clustering systems can serve as potential molecular antennae in creation of effective light-harvesting devices and synthetic elaboration of new multichromophoric dendrimer system is therefore of great significance.[8–11] In the present work, we intend to investigate the possibility of accessing higher-generation dendritic architectures as a logical extension of the synthetic methodology, which allows us to generate a variety of dendrimer systems with higher local density of light-collecting units. Despite our intention, incorporation of the anthracene groups into the dendritic frameworks was initially hampered by the low branching configurations.[12] Accordingly, key to the successful implementation of the synthetic plan is utilization of junction units for introduction of branching elements into the anthracene nucleus, converting it to the branched building blocks. Based on this functionalization strategy, we established a simple methodology for construction of four types of second-generation dendritic architectures **3B**, **3L**, **4B**, and **4L** (Fig. 1) as representative members of the higher-generation

Keywords: Dendrimer; Anthracene; Fluorescence; Intramolecular energy migration; Time-resolved fluorescence decay measurement.
* Corresponding author. Tel./fax: +81 53 478 1621;
e-mail: tmtakah@ipc.shizuoka.ac.jp

0040–4020/$ - see front matter © 2006 Elsevier Ltd. All rights reserved.
doi:10.1016/j.tet.2006.01.024

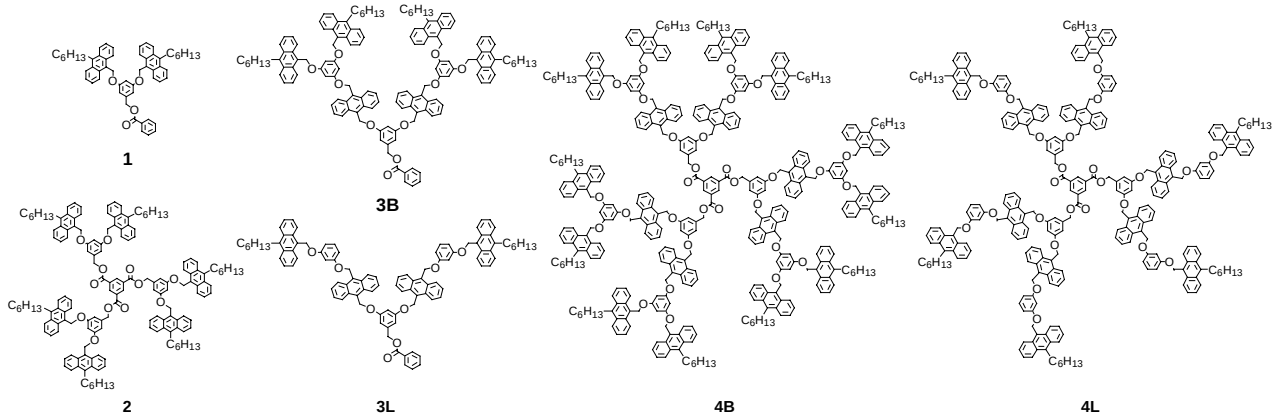

Figure 1. Structures of dendritic molecules **1**–**4**.

family, where we shall occasionally employ the letters **B** and **L** to designate branching and linear geometries of multichromophoric substituents, respectively. Along with the synthetic achievement and property investigation of the dendritic compounds, we disclose photophysical characteristics for energy delocalization functionalities of the new multichromophoric systems.

2. Results and discussion

Our previous report has shown that direct coupling of variously substituted 10-alkyl-9-anthryl chlorides and polyphenolic linkers **5** and **6** was viable for the syntheses of the lowest dendritic generations.[7] In an attempt to apply this methodology to the second-generation dendritic architectures, our attention focused on preparations of requisite anthryl chlorides **7B** and **7L** carrying additional anthracene functionalities at the C10-position of the anthracene ring system (Fig. 2).

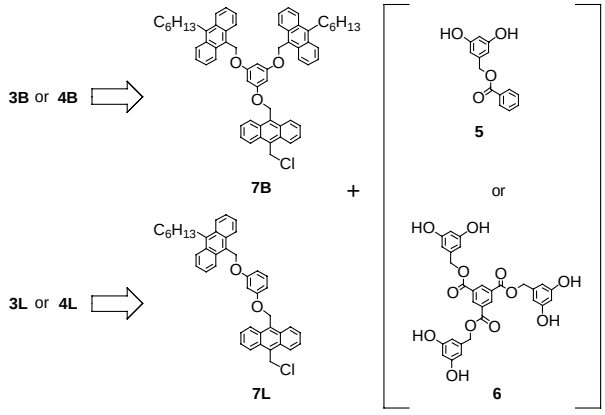

Figure 2. Retrosynthetic analyses.

Our approach to the dendritic architectures started with preparation of an asymmetrically 9,10-disubstituted anthracene through site-selective bromination. In general, the course of free radical bromination with *N*-bromosuccinimide is influenced profoundly by local electron density of active methylene groups.[13] When 9-acetoxy-10-methylanthracene **8** was employed as the reactant, hydrogen abstraction took place predominantly at the methyl group adjacent to the anthracene ring as a result of deactivation of the benzylic counterparts by neighboring acetoxy group, giving rise to 9-acetoxy-10-bromomethylanthracene **9** in 95% yield (Scheme 1).

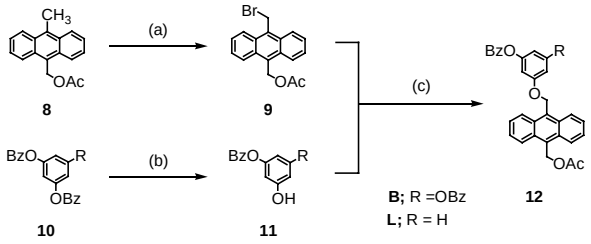

Scheme 1. Syntheses of **12**. Conditions: (a) NBS, AIBN, $CHCl_3$, reflux, 95%; (b) Cs_2CO_3, DME, reflux, **11B** (79%), **11L** (72%); (c) 18-crown-6, K_2CO_3, DMF, 55 °C, **12B** (90%), **12L** (92%).

For the preparation of branching skeletal series, the corresponding junction unit was synthesized by selective removal of benzoyl groups from phloroglucinol tribenzoate **10B**.[14] The controlled hydration of **10B** was accomplished with cesium carbonate under an anhydrous condition to give 3,5-dibenzoyloxyphenol **11B** in 79% yield. This compound possesses one phenolic hydroxyl group available for nucleophilic coupling with **9**, leading to **12B** in 90% yield (Scheme 2).

Deprotection of two remaining benzoyl groups in **12B** using excess *n*-butylamine gave bisphenolic derivative **13B** in 81% yield without affecting the terminal acetoxy group.[15] The subsequent transformation of **13B** into **14B** was conducted by the established protocol for the synthesis of first-generation dendrons.[7] As for an endcapping reagent required for this reaction, 10-(*n*-hexyl)-9-anthryl chloride was selected due to the fact that attaching the long alkyl side chain on the peripheral anthracene groups enhanced solubility of the resulting dendrimer in a variety of organic solvents.[7] Thus, the coupling between **13B** and 2 mol equiv of the anthryl chloride underwent efficient ether bond formation providing **14B** in 60% yield. The acetyl endgroup of **14B** underwent efficient deprotection by hydrolysis with sodium methoxide in methanol solution to give the corresponding alcohol **15B**

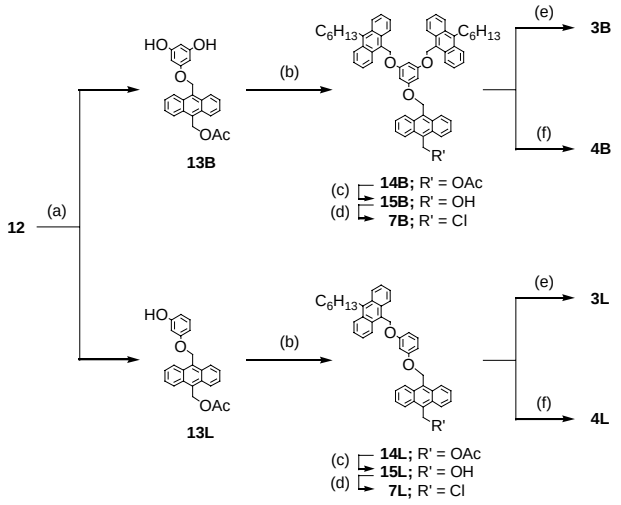

Scheme 2. Syntheses of **3** and **4**. Conditions: (a) *n*-$BuNH_2$, THF, reflux, **13B** (81%), **13L** (85%); (b) 10-(*n*-hexyl)-9-anthryl chloride, 18-crown-6, K_2CO_3, DMF, 55 °C, **14B** (84%), **14L** (94%); (c) CH_3ONa, 1:1 THF/CH_3OH, reflux, **15B** (95%), **15L** (92%); (d) MsCl, LiCl, DMAP, Et_3N, THF, rt, **7B** (87%), **7L** (91%); (e) **5**, 18-crown-6, K_2CO_3, DMF, 55 °C, **3B** (75%), **3L** (69%); (f) **6**, 18-crown-6, K_2CO_3, DMF, 55 °C, **4B** (57%), **4L** (48%).

in 95% yield. In the final step of the reaction sequence, we attempted to convert the hydroxyl group of **15B** by generation of the corresponding mesylate followed by in situ displacement reaction in the presence of excess lithium chloride to the desired anthryl chloride **7B** in 87% yield. A similar set of reactions was employed to prepare the linear segment **7L**, where a resorcinol moiety was incorporated as another junction unit in place of the phloroglucinol building component in **7B**. Starting from resorcinol dibenzoate **10L**, all synthetic reactions proceeded with good to excellent yields (72–94%) and gave rise to **7L** through six sequential steps.

Subsequent covalent attachment of **7B** and **7L** to two types of the polyphenolic linkers **5** and **6**, available from previous works,[7] was facilitated by the successive nucleophilic substitution reactions at the multiple sites, giving rise to the second-generation dendritic molecules **3B** (75%), **3L** (69%), **4B** (57%), and **4L** (48%), respectively. All these compounds were fully characterized by a range of spectroscopies along with elemental analyses. For instance, simplicity of the ^1H and ^{13}C NMR spectra is consistent with the highly symmetric structures. In particular, the ^1H NMR of **4B** and **4L** exhibited low-field singlets at 8.95 and 9.01 ppm, respectively, due to aromatic protons attached to the cores, indicating that all three dendritic branching units of this molecule should be chemically equivalent. The molecular weights of these compounds were examined by electrospray ionization mass spectrometry (ESI-MS).[16] This allowed a qualitative analysis of **3B** exhibiting the parent ion peaks at *m/z* 2020.9, attributable to $[M+Na]^+$ (calcd *m/z* 2020.0), with a calculated isotopic distribution pattern (Fig. 3a). During this measurement, three minor peaks were simultaneously observed at *m/z* 2036.9, 2052.9, and 2069.0 possibly due to oxidized molecular ions (calcd *m/z* 2036.0 $[M+NaO]^+$, 2052.0 $[M+NaO_2]^+$, and 2068.0 $[M+NaO_3]^+$, respectively). This observation indicates the poly(anthryl ether) dendritic compounds are very susceptible to oxidative degradation under the instrumental

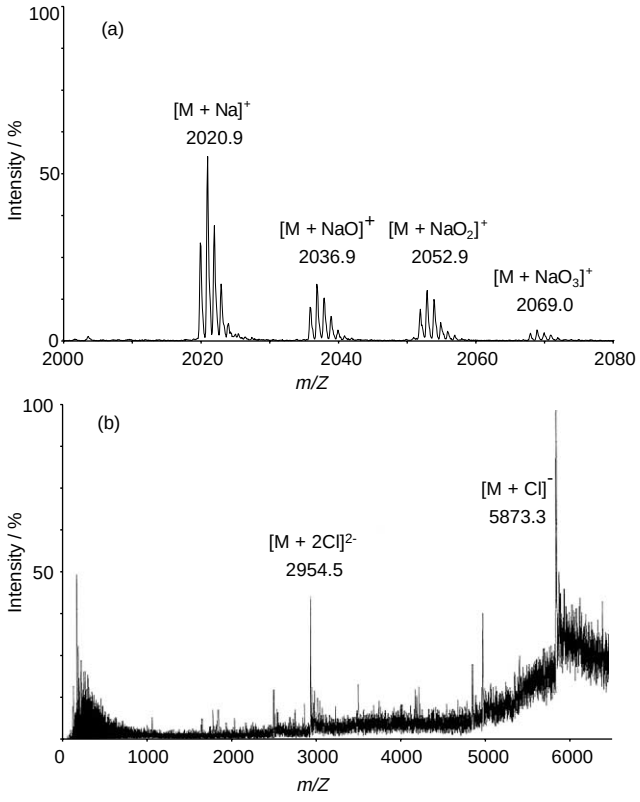

Figure 3. (a) ESI-MS spectrum of **3B**. (b) CSI-MS spectrum of **4B**.

conditions of operation. In fact, the analogous dendron **3L** provided predominantly molecular ion peaks at *m/z* 1471.5 as an oxidized substrate $[M+NaO_2]^+$ (calcd *m/z* 1471.6) under the identical experimental condition. On the other hand, the dendrimers **4B** and **4L** did not exhibit any parent ion peak by similar ESI-MS measurements and fragmented exclusively to stabilized anthryl ionic species. Further investigations by coldspray ionization mass spectral (CSI-MS) technique provided compelling evidence for the formation of **4B** and **4L**.[17] The CSI-MS analysis of **4B** exhibited singly and doubly charged molecular ion peaks at *m/z* 5873.3 $[M+Cl]^-$ (calcd 5874.8) and 2954.5 $[M+2Cl]^{2-}$ (calcd 2954.9), respectively (Fig. 3b), while **4L** gave only a singly charged ion peak at *m/z* 4131.8 $[M+Cl]^-$ (calcd 4131.8). These results clearly indicate the success of our synthetic strategy achieving complete coverage of the dendrimer backbones.

Alternatively, the molecular weights of these materials were also estimated using a relative method such as gel permeation chromatography (GPC) calibrated with polystyrene standards. In chloroform solutions, all dendritic compounds exhibited sharp and symmetrical peaks at discrete retention times with low polydispersity values ($M_w/M_n<1.01$) that should be in the range typically found for unified dendrimers (Table 1). Figure 4 demonstrates that either a series of dendrons **1**, **3B**, and **3L** or a series of dendrimers **2**, **4B**, and **4L** provided almost monomodal distributions fitted well with the linear polystyrene series in the correlation diagram, where observed retention volumes of all dendritic compounds exhibited a linear dependence on logarithmic numbers of the averaged molecular weights. Table 1 presents the molecular weights of the dendrimers

Table 1. Structural details, GPC results, and maximum solubilities of **1–4**

Entry	Number of anthracene units	Formula	M_w/M_n[a]	Nominal M_w	M_w	c (mol/L)[b]
1	2	$C_{56}H_{56}O_4$	1.001	792	746	3.8×10^{-1}
2[c]	6	$C_{156}H_{156}O_{12}$	1.004	2221	2074	1.0×10^{-2}
3B	6	$C_{142}H_{132}O_{10}$	1.002	1997	2258	1.3×10^{-2}
3L	4	$C_{100}H_{88}O_8$	1.001	1417	1553	5.9×10^{-3}
4B	18	$C_{414}H_{384}O_{30}$	1.003	5835	5460	6.8×10^{-4}
4L	12	$C_{288}H_{252}O_{24}$	1.008	4094	3940	1.4×10^{-5}

[a] Calibrated with narrow-dispersity polystyrene standards.
[b] Maximum concentrations dissolved in chloroform at 20 °C.
[c] See Ref. 7.

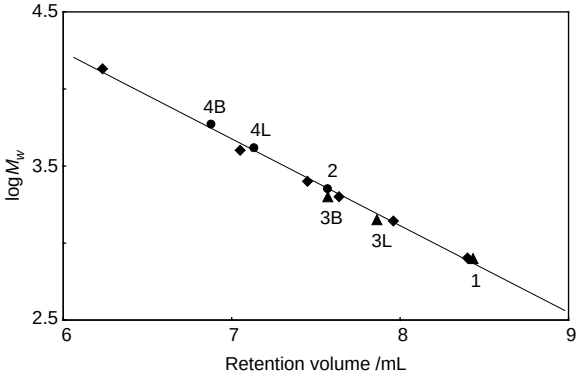

Figure 4. Semilogarithmic plot of average molecular weights (M_w) versus GPC retention volumes for polystyrene standards (◆), dendrons (▲), and dendrimers (●).

(M_w) determined by the GPC analyses calibrated with the polystyrene standards. As can be seen in Table 1, the estimated values for both series are satisfactorily close to the nominal molecular weights with small differences less than 13%, indicating this analytical experiment provides reliable information on the approximate molecular sizes.

The degree of branching in the three-dimensional dendritic skeletal frameworks allows for direct control of solubility in common organic solvents. Table 1 also includes maximum solubilities of the dendritic macromolecules in chloroform solutions, which were determined by dissolving the samples in chloroform and measuring their UV absorption maxima around 380 nm. From these data, impressive differences were observed in the solubilities between the branching (B) and linear (L) dendritic architectures. In comparison, the maximum solubility of **3B** was increased by 2.2-fold compared with **3L**, while **4B** displayed significantly enhanced solubility as large as about 49-fold relative to **4L**. It should be noted that the branching skeletal systems offer the advantage of higher solubility although they contain large numbers of insoluble anthracene moieties in confined molecular spaces. These solubilization phenomena may be understood on the basis of net lipophilic properties of the molecules functionalized by the alkyl solubilizing groups. In general, the branching dendritic architectures are designed to bring greater number of peripheral groups in defined geometries than the linear systems, thus reinforcing the extent of surface functionalization of the dendritic shells. For the case of our model systems, such a structural aspect may result in an increase of incorporation ratio of the terminal solubilizing groups within the branching dendritic frameworks, which should significantly enhance solubilities of the resulting compounds. Consequently, the experimental results obtained are in good agreement with this proposal, demonstrating that the branching geometry of the macromolecular systems strongly influences the intrinsic maximum solubility for the dendritic architectures.

In an effort to gain insight into the scope of photophysical properties, we investigated absorption and fluorescence behavior of the two analogous series of the new dendritic molecules **3–4**. All these compounds showed comparable absorption profiles giving three intense peaks at around 360, 380, and 400 nm attributed to anthracene absorptions whose molar absorption coefficients are approximately proportional to the number of anthracene units. On the other hand, individual dendritic molecules behaved differently with respect to the fluorescence spectroscopic features. Figure 5 shows a series of steady-state fluorescence emission spectra of all the dendritic architectures **1–4** upon excitation at 378 nm. As illustrated, the emission spectra of the both dendrons **3B** and **3L** displayed vibronic fine-structures with two sharp bands at around 410 and 430 nm and shoulders in the longer wavelength region, resembling closely the emission spectrum of the first-generation analogue **1** with diminished intensity levels. Furthermore, the two dendrimers **4B** and **4L** exhibited slightly red-shifted and less efficient emissions relative to the first-generation analogue **2**.

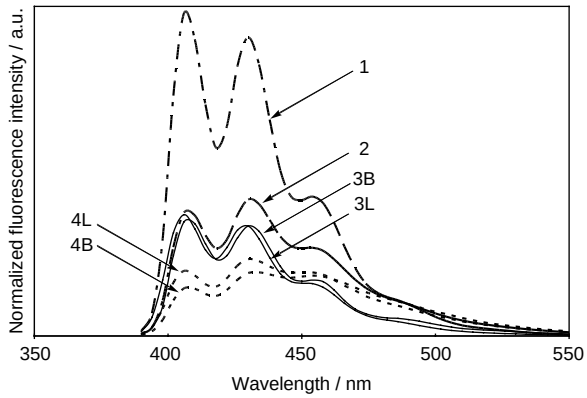

Figure 5. Steady-state fluorescence spectra of **1** and **2** (dashed lines), **3B** and **3L** (solid lines), and **4B** and **4L** (dotted lines) in chloroform solutions. The spectra were obtained by excitation at 378 nm and normalized to the same optical density at the excitation wavelength. All measurements were conducted in sufficiently low concentrations ($10^{-8}\sim10^{-7}$ M) of the analytes to exclude the possibilities of intermolecular interactions.

Indeed, the second-generation **3**–**4** exhibited weaker emission bands than the first-generation **1**–**2** as expressed by lower fluorescence quantum yields (Table 2). This suggested the new dendritic molecules allowed fast energy delocalization driven by the chromophore cluster effects that were strongly dependent on the branching molecular geometry and the number of chromophores present in the dendritic systems.[18] At this point, it is of interest to note that **3B** showed a significantly lowered fluorescence quantum efficiency in comparison to that of its geometric isomer **2**, while the estimated values for the second-generation family were substantially unaffected by the number of chromophores incorporated within the dendritic frameworks. The observed dependence of the quantum yields on the molecular geometry can be rationalized in terms of interchromophore separations defined by differences in local packing density of the chromophoric groups, which should be the most important factor in governing energy migration rates.[19] It is well accepted that the energy transfer rates due to either electron exchange (Dexter) mechanism through collision interactions or dipole–dipole (Förster) mechanism through Coulombic interactions are extremely influenced by the average distances between the donor and acceptor.[20,21] This rationale suggests a tentative conclusion that these two mechanisms may dominate the energy migration processes in the dendritic anthracene arrays. However, these mechanistic possibilities cannot be substantially distinguished by uncertainties in interchromophoric distances because of inherent flexibility in the dendrimer conformations.

Table 2. Absorption and fluorescence maxima, and fluorescence quantum yields of **1**–**4**

Entry	λ_{abs} (nm)	λ_F (nm)	Φ_F
1[a]	360, 379, 400	410, 430, 454	0.36
2[a]	360, 379, 400	409, 433, 454	0.20
3B	358, 378, 398	409, 432, 456	0.13
3L	357, 375, 396	406, 430, 450	0.14
4B	359, 378, 399	409, 434, 458	0.13
4L	358, 377, 397	406, 430, 450	0.14

[a] See Ref. 7.

To investigate energy migration dynamics of the second-generation dendrimer systems, time-resolved fluorescence decay measurements were performed on the largest dendrimer **4B** as a representative example of the second-generation dendritic architectures. Figure 6 illustrates the fluorescence intensity traces of **1**, **2**, and **4B**, which demonstrated **4B** decayed faster than the first-generations **1** and **2** following a multiexponential curve.[22] An attempt to analyze the data of **4B** with a triexponential function gave a satisfactory fit with lifetimes of 5.6 ns (44%), 1.6 ns (33%), and 0.37 ns (23%). As demonstrated previously for first-generation analogues carrying ethyl substituents at the peripheral positions, the decay profile for **1** followed satisfactorily a monoexponential function with a decay component of 5.6 ns, while the decay for **2** was well fitted with a biexponential yielding two components of 5.6 ns (68%) and 1.6 ns (32%).[7] In comparison, the two slower decay components of 5.6 and 1.6 ns found in **4B** can be assigned to originate from the first-generation dendrimer **2**, which may include the dynamic character of the bichromophoric dendron **1** with the longest decay component of 5.6 ns. During the course of our studies, we found that all the three multichromophoric dendritic systems examined may share a common mechanistic feature with respect to the energy migration channels and thus the second-generation dendrimer **4B** may cover all the decaying elements of the constituent molecules. Based on this consideration, the fast decay component of 0.37 ns observed for **4B** can be deduced to be a newly introduced energy migration channel caused by the densely multichromophoric array of the second-generation dendrimer.[23]

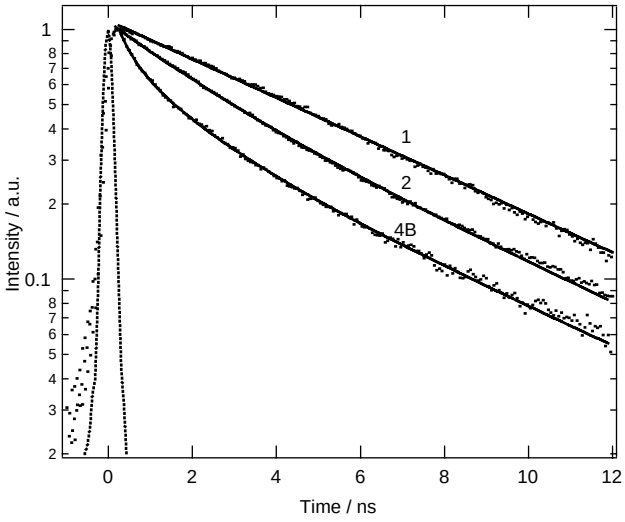

Figure 6. Fluorescence decay profiles at 433 nm of **1**, **2**, and **4B** in THF solutions (excitation at 355 nm).

3. Conclusion

In conclusion, we described simple methodologies that allowed ready access to the four types of second-generation dendritic architectures containing up to 18 anthracene units either within their structural interior or at their periphery. The synthetic procedure presented here provides a promising strategy to construct the higher-generation dendritic architectures, which realizes denser arrays of anthracene groups in well-defined molecular spaces. The developed dendritic molecules have been shown to undergo the intramolecular energy migration extending over a large part of the dendritic architectures. Finally, the present multichromophoric systems represent a potential light-harvesting antenna that can capture photons and transfer them to neighboring photoactive units within supramolecular environments.

4. Experimental

4.1. General

All solvents and reagents were of reagent grade quality from Wako Pure Chemicals used without further purification. The ^{1}H and ^{13}C nuclear magnetic resonance (NMR) spectra operating at the frequencies of 300 and 75 MHz, respectively, were recorded on a JEOL JNM-AL300 spectrometer

in chloroform-*d* ($CDCl_3$) or acetone-d_6 ($(CD_3)_2CO$). Chemical shifts are reported in parts per million (ppm) relative to TMS and the solvent used as internal standards, and the coupling constants are reported in hertz (Hz). Fourier transform infrared (FT-IR) spectra were recorded on a JASCO FT/IR-410 spectrometer as KBr disks. Absorption spectra were recorded on a JASCO model V-570 UV–vis–NIR spectrophotometer. Fluorescence spectra were measured on a Hitachi F-4500 spectrofluorometer. Melting points were measured with a Yanaco MP-S3 melting point apparatus. Fast atom bombardment (FAB) mass measurements were performed by a JASCO JMS-HX110A spectrometer using a 3-nitrobenzyl alcohol matrix. Electrospray ionization-time-of-flight (ESI-TOF) mass spectra of **3B**, **3L**, and **9** were recorded on a Micromass LCT mass spectrometer KB 201. Coldspray ionization mass (CSI-MS) spectral measurements of **4B** and **4L** were performed by two-sector (BE) mass spectrometer (JMS-700, JEOL) equipped with a cold-spray ionization (CSI) source. Elemental analyses were obtained from Thermo Flash EA 1112 instrument. Gel permeation chromatography (GPC) was performed on a system consisting of a JASCO model 880-PU pump at a flow rate of 0.5 mL/min and JASCO 875-UV absorbance detector (254 nm) equipped with a Shodex K-802.5 column, where chloroform was used as mobile phase. Time-resolved fluorescence decay measurements of **1**, **2**, and **4B** were performed on a system consisting of a Hamamatsu C5094 imaging spectrograph and a B. M. Industries 5022 D. PS. DP.10 passively/actively mode-locked Nd:YAG laser employing the third harmonic at 355 nm. These measurements were conducted in THF solutions. The decays were fitted with the least-squares (LS) method to evaluate the fluorescence lifetimes. The quality of the fits has been judged from the estimated values and residuals. Preparative high-performance liquid chromatography (HPLC) was performed on a Japan Analytical Industry LC-918 recycling system. Samples of first-generation dendron **1**, dendrimer **2**, multibranched polyphenolic linkers **5** and **6**, 9-acetoxymethyl-10-methylanthracene **8**, resorcinol dibenzoate **10L**, 3-benzoyloxyphenol **11L**, and 10-(*n*-hexyl)-9-anthryl chloride were prepared by the procedures reported in the previous publications.[7,14] Synthetic intermediates of phloroglucinol tribenzoate **10B** and 3,5-dibenzoyloxyphenol **11B** were prepared by alternative approaches to improve reaction yields for comparison with published procedures.[24] The fluorescence quantum yields of **3B**, **3L**, **4B**, and **4L** were determined in comparison to those of **1** and **2** in chloroform solutions, which were employed as standards.

4.1.1. Synthetic procedure for 9. A solution containing **8** (0.86 g, 3.26 mmol), *N*-bromosuccinimide (0.57 g, 3.22 mmol), and 2,2′-azobisisobutyronitrile (0.027 g, 0.16 mmol) in chloroform (100 mL) was heated to reflux stirring under argon atmosphere. After 4 h, the reaction mixture was cooled to room temperature, and then the solvent was removed in vacuo. This resulting solid was dissolved in DMF (20 mL), and the solution was poured into excess water to precipitate the product. The precipitate was collected by filtration, intensively washed with water, and dried in a vacuum to afford a yellow solid. After complete vacuum drying, the resulting solid was purified by recrystallization from chloroform–hexane, affording **9** (1.06 g, 95%) as a yellow powder: mp 192–194 °C; IR (KBr) 1730 cm^{-1} (C=O); MS (ESI, positive) *m/z* 365 (*MNa*+); ^1H NMR ($CDCl_3$) δ 2.09 (s, 3H, CH_3), 5.52 (s, 2H, CH_2Br), 6.14 (s, 2H, CH_2O), 7.58–7.69 (m, 4H, Ar*H*), 8.34–8.41 (m, 4H, Ar*H*); ^{13}C NMR ($CDCl_3$) δ 20.9 (CH_3), 26.6 (CH_2), 58.8 (CH_2), 124.2 (*C*H), 124.8 (*C*H), 126.5 (*C*H), 126.6 (*C*H), 128.7 (*C*), 129.4 (*C*), 130.3 (*C*), 131.0 (*C*), 171.1 (*C*). Anal. Calcd for $C_{18}H_{15}BrO_2$: C, 62.99; H, 4.41; N, 0.00. Found: C, 62.69; H, 4.68; N, 0.07.

4.1.2. Synthetic procedure for 10B. Commercially available phloroglucinol dihydrate was dried in a vacuum oven for 1 day prior to use. To a solution containing the dehydrated phloroglucinol (3.69 g, 0.0293 mol) and triethylamine (24.4 mL, 0.175 mol) in THF (10 mL), a solution of benzoyl chloride (11.8 mL, 0.102 mol) in THF was added dropwise under vigorous stirring at 0 °C. The reaction was allowed to continue for additional 3 h at room temperature. The reaction mixture was then quenched by slow addition of diluted HCl (3.0 mol/L, 100 mL) to precipitate the product. The precipitate was collected by filtration, intensively washed with water, and dried in a vacuum to afford a white solid. Purification of the resulting solid by recrystallization from chloroform solution gave **10B** (10.0 g, 78%) as a white powder. This compound was identified by comparison of the ^1H NMR chemical shifts with the literature data.[24]

4.1.3. Synthetic procedure for 11B. The synthetic procedure for **11B** was achieved by following a new method. A solution containing **10B** (3.03 g, 6.92 mmol) and cesium carbonate (1.80 g, 5.52 mmol) in anhydrous dimethoxyethane (50 mL) was heated to reflux with vigorous stirring under argon atmosphere. After 18 h, the reaction mixture was cooled to room temperature, quenched by slow addition of diluted HCl (3.0 mol/L, 40 mL), and then extracted twice with ethyl acetate (30 mL). The combined organic layers were washed with water (20 mL), saturated aqueous $NaHCO_3$ (20 mL), and brine (20 mL). The organic layer was separated, dried over anhydrous Na_2SO_4, filtered, and concentrated in vacuo. The residue was dissolved in chloroform (30 mL), and the solution was filtered through Celite to remove the remaining starting material. After the filtrate was concentrated in vacuo, the residue was purified by silica-gel column chromatography (chloroform as eluent) to give **11B** (1.83 g, 79%) as a white powder. This compound was identified by comparison of the ^1H NMR chemical shifts with the literature data.[24]

4.1.4. Synthetic procedure for 12B. A solution containing **9** (0.36 g, 1.05 mmol), **11B** (0.32 g, 0.96 mmol), potassium carbonate (0.20 g, 1.44 mmol), and 18-crown-6 (0.13 g, 0.49 mmol) in DMF (5 mL) was heated at 55 °C with stirring under argon atmosphere. After 4 h, the reaction mixture was cooled to room temperature, and poured into saturated ammonium chloride solution to precipitate the product. The precipitate was collected by filtration, intensively washed with water, and dried in a vacuum to afford a pale yellow solid. Purification of the residue by silica-gel column chromatography (70% chloroform, 30% hexane) gave **12B** (0.52 g, 90%) as a pale yellow powder. Further purification was achieved by recrystallization from

$CHCl_3$–methanol solution: mp 188–190 °C; IR (KBr) 1597 cm^{-1} (C=C), 1738 cm^{-1} (C=O); MS (FAB, positive) *m/z* 596 (*M*+), 597 (*MH*+); ^1H NMR ($CDCl_3$) δ 2.09 (s, 3H, CH_3), 5.99 (s, 2H, CH_2), 6.18 (s, 2H, CH_2), 6.91 (t, *J*=2.0 Hz, 1H, Ar*H*), 6.99 (d, *J*=2.0 Hz, 2H, Ar*H*), 7.49–7.54 (m, 4H, Ar*H*), 7.58–7.64 (m, 6H, ArH), 8.19–8.22 (m, 4H, Bz*H*), 8.32–8.42 (m, 4H, Ar*H*); ^{13}C NMR ($CDCl_3$) δ 20.9 (*C*H_3), 58.8 (*C*H_2), 63.3 (*C*H_2), 106.4 (*C*H), 108.9 (*C*H), 124.7 (*C*H), 126.3 (*C*H), 126.4 (*C*H), 128.5 (*C*), 128.6 (*C*H), 128.8 (*C*), 129.3 (*C*), 130.2 (*C*H), 130.8 (*C*), 133.8 (*C*H), 152.2 (*C*), 160.3 (*C*), 164.8 (*C*), 171.2 (*C*). Anal. Calcd for $C_{38}H_{28}O_7$: C, 76.50; H, 4.73; N, 0.00. Found: C, 76.19; H, 4.97; N, 0.00.

4.1.5. Synthetic procedure for 12L. A solution containing **9** (1.43 g, 4.18 mmol), **11L** (0.81 g, 3.80 mmol), potassium carbonate (0.79 g, 5.72 mmol), and 18-crown-6 (0.50 g, 1.89 mmol) in DMF (8 mL) was heated at 55 °C with stirring under argon atmosphere. After 4 h, the reaction mixture was cooled to room temperature, and poured into saturated ammonium chloride solution to precipitate the product. The precipitate was collected by filtration, intensively washed with water, and dried in a vacuum. Purification by recrystallization from $CHCl_3$–hexane solution gave **12L** (1.66 g, 92%) as a pale yellow solid: mp 234–236 °C; IR (KBr) 1603 cm^{-1} (C=C), 1736 cm^{-1} (C=O); MS (FAB, positive) *m/z* 476 (*M*+), 477 (*MH*+); ^1H NMR ($CDCl_3$) δ 2.09 (s, 3H, COCH_3), 5.95 (s, 2H, CH_2), 6.17 (s, 2H, CH_2), 6.91–6.95 (m, 1H, Ar*H*), 7.02–7.06 (m, 2H, Ar*H*), 7.39–7.44 (m, 2H, Ar*H*), 7.49–7.66 (m, 7H, Ar*H*), 8.21–8.24 (m, 2H, Bz*H*), 8.30–8.41 (m, 4H, Ar*H*); ^{13}C NMR (CDCl*3*) δ 21.0 (*C*H_3), 58.8 (*C*H_2), 63.0 (*C*H_2), 108.5 (*C*H), 112.7 (*C*H), 114.6 (*C*H), 124.6 (*C*H), 124.7 (*C*H), 126.3 (*C*H), 128.6 (*C*H), 128.7 (*C*), 128.9 (*C*), 129.5 (*C*), 130.1 (*C*H), 130.2 (*C*H), 130.7 (*C*), 130.8 (*C*), 133.7 (*C*H), 152.1 (*C*), 160.1 (*C*), 165.2 (*C*), 171.2 (*C*). Anal. Calcd for $C_{31}H_{24}O_5$: C, 78.14; H, 5.08; N, 0.00. Found: C, 78.03; H, 5.11; N, 0.00.

4.1.6. Synthetic procedure for 13B. A solution containing **12B** (0.68 g, 1.14 mmol) and *n*-butylamine (2.26 mL, 22.9 mmol) in THF (15 mL) was heated to reflux with stirring under argon atmosphere. After 18 h, the reaction mixture was cooled to room temperature, and concentrated in vacuo. Purification of the residue by silica-gel column chromatography (67% hexane, 33% ethyl acetate) and recrystallization from hexane–ethyl acetate solution gave **13B** (0.36 g, 81%) as a pale yellow powder: dp 186–188 °C; IR (KBr) 1606 cm^{-1} (C=C), 1732 cm^{-1} (C=O), 3383 cm^{-1} (OH); MS (FAB, positive) *m/z* 388 (*M*+), 399 (*MH*+); ^1H NMR ($(CD_3)_2CO$) δ 2.03 (s, 3H, CH_3), 5.97 (s, 2H, CH_2), 6.09 (t, *J*=2.1 Hz, 1H, Ar*H*), 6.19 (s, 2H, CH_2), 6.15 (d, *J*=2.1 Hz, 2H, Ar*H*), 7.59–7.67 (m, 4H, Ar*H*), 8.31 (br s, 2H, O*H*), 8.41–8.51 (m, 4H, Ar*H*); ^{13}C NMR ($(CD_3)_2CO$) δ 20.8 (*C*H_3), 59.2 (*C*H_2), 63.2 (*C*H_2), 94.9 (*C*H), 97.0 (*C*H), 125.6 (*C*H), 125.9 (*C*H), 127.0 (*C*H), 127.1 (*C*H), 129.8 (*C*), 131.0 (*C*), 131.6 (*C*), 131.7 (*C*H), 160.3 (*C*), 162.3 (*C*), 171.1 (*C*). Anal. Calcd for $C_{24}H_{20}O_5$: C, 74.21; H, 5.19; N, 0.00. Found: C, 73.96; H, 5.35; N, 0.03.

4.1.7. Synthetic procedure for 13L. A solution containing **12L** (0.71 g, 1.49 mmol) and *n*-butylamine (1.47 mL, 14.9 mmol) in THF (20 mL) was heated to reflux with stirring under argon atmosphere. After 18 h, the reaction mixture was cooled to room temperature, and concentrated in vacuo. Purification of the residue by silica-gel column chromatography (60% hexane, 40% ethyl acetate) and recrystallization from hexane–ethyl acetate solution gave **13L** (0.47 g, 85%) as a pale yellow powder: mp 190–191 °C; IR (KBr) 1591 cm^{-1} (C=C), 1707 cm^{-1} (C=O), 3411 cm^{-1} (OH); MS (FAB+) *m/z* 372 (*M*+), 373 (*MH*+); ^1H NMR ($(CD_3)_2CO$) δ 2.04 (s, 3H, COCH_3), 6.02 (s, 2H, CH_2), 6.19 (s, 2H, CH_2), 6.51–6.55 (m, 1H, Ar*H*), 6.64–6.71 (m, 2H, Ar*H*), 7.15–7.21 (m, 1H, Ar*H*), 7.58–7.66 (m, 4H, Ar*H*), 8.38 (s, 1H, O*H*), 8.41–8.50 (m, 4H, Ar*H*); ^{13}C NMR ($(CD_3)_2CO$) δ 20.8 (*C*H_3), 59.2 (*C*H_2), 63.3 (*C*H_2), 103.3 (*C*H), 106.8 (*C*H), 109.3 (*C*H), 125.7 (*C*H), 125.9 (*C*H), 127.0 (*C*H), 127.1 (*C*H), 129.8 (*C*), 130.9 (*C*H), 131.6 (*C*), 131.7 (*C*), 159.7 (*C*), 161.6 (*C*), 171.1 (*C*). Anal. Calcd for $C_{24}H_{20}O_4$: C, 77.40; H, 5.41; N, 0.00. Found: C, 77.28; H, 5.29; N, 0.00.

4.1.8. Synthetic procedure for 14B. A solution containing **13B** (0.26 g, 0.67 mmol), 10-(*n*-hexyl)-9-anthryl chloride (0.46 g, 1.48 mmol), potassium carbonate (0.25 g, 1.81 mmol), and 18-crown-6 (0.18 g, 0.68 mmol) in DMF (8 mL) was heated at 55 °C with stirring under argon atmosphere. After 4 h, the reaction mixture was cooled to room temperature, and poured into saturated ammonium chloride solution to precipitate the product. The precipitate was collected by filtration, intensively washed with water, and dried in a vacuum to afford a pale yellow solid. Purification of the residue by silica-gel column chromatography (70% chloroform, 30% hexane) gave **14B** (0.53 g, 84%) as a pale yellow power. Further purification was achieved by recrystallization from $CHCl_3$–methanol solution: mp 223–225 °C; IR (KBr) 1587 cm^{-1} (C=C), 1739 cm^{-1} (C=O); MS (FAB, positive) *m/z* 936 (*M*+), 937 (*MH*+); ^1H NMR ($CDCl_3$) δ 0.91 (t, *J*=7.1 Hz, 6H, $(CH_2)_5CH_3$), 1.31–1.42 (m, 8H, $(CH_2)_3(CH_2)_2CH_3$), 1.56–1.61 (m, 4H, $(CH_2)_2CH_2(CH_2)_2CH_3$), 1.75–1.85 (m, 4H, $CH_2CH_2(CH_2)_3CH_3$), 3.61 (t, *J*=8.3 Hz, 4H, CH_2(CH_2)$_4$-CH_3), 5.88 (s, 4H, CH_2), 5.90 (s, 2H, CH_2), 6.16 (s, 2H, CH_2OAc), 6.66 (d, *J*=2.1 Hz, 2H, Ar*H*), 6.69 (t, *J*=2.1 Hz, 1H, Ar*H*), 7.48–7.60 (m, 12H, Ar*H*), 8.30–8.39 (m, 12H, Ar*H*); ^{13}C NMR ($CDCl_3$) δ 14.1 (*C*H_3), 21.0 (*C*H_3), 22.7 (*C*H_2), 28.5 (*C*H_2), 30.1 (*C*H_2), 31.4 (*C*H_2), 31.8 (*C*H_2), 50.8 (*C*H_2), 62.8 (*C*H_2), 63.0 (*C*H_2), 94.9 (*C*H), 95.0 (*C*H), 124.7 (*C*H), 124.8 (*C*H), 125.1 (*C*H), 125.2 (*C*H), 126.1 (*C*H), 126.3 (*C*H), 128.6 (*C*), 129.2 (*C*), 129.4 (*C*), 130.8 (*C*), 130.9 (*C*), 131.0 (*C*), 138.1 (*C*), 161.2 (*C*), 161.4 (*C*), 171.8 (*C*). Anal. Calcd for $C_{66}H_{64}O_5$: C, 84.58; H, 6.88; N, 0.00. Found: C, 84.23; H, 7.10; N, 0.07.

4.1.9. Synthetic procedure for 14L. A solution containing **13L** (0.57 g, 1.53 mmol), 10-(*n*-hexyl)-9-anthryl chloride (0.53 g, 1.71 mmol), potassium carbonate (0.30 g, 2.17 mmol), and 18-crown-6 (0.20 g, 0.76 mmol) in DMF (8 mL) was heated at 55 °C with stirring under argon atmosphere. After 4 h, the reaction mixture was cooled to room temperature, and poured into saturated ammonium chloride solution to precipitate the product. The precipitate was collected by filtration, intensively washed with water, and dried in a vacuum to afford a pale yellow solid. Purification of the residue by recrystallization from

$CHCl_3$–methanol solution gave **14L** (0.93 g, 94%) as a pale yellow power: mp 198–200 °C; IR (KBr) 1587 cm^{-1} (C=C), 1732 cm^{-1} (C=O); MS (FAB+) *m/z* 646 (*M*+), 647 (*MH*+); ^{1}H NMR ($CDCl_3$) δ 0.92 (t, *J*=6.8 Hz, 3H, $(CH_2)_5CH_3$), 1.35–1.43 (m, 4H, $(CH_2)_3(CH_2)_2CH_3$), 1.54–1.63 (m, 2H, $(CH_2)_2CH_2(CH_2)_2CH_3$), 1.79–1.82 (m, 2H, $CH_2CH_2(CH_2)_3CH_3$), 3.64 (t, *J*=7.8 Hz, 2H, $CH_2(CH_2)_4CH_3$), 5.95 (s, 2H, CH_2), 5.97 (s, 2H, CH_2), 6.19 (s, 2H, $CH_2O(C=O)CH_3$), 6.84–6.96 (m, 3H, Ar*H*), 7.35–7.41 (m, 1H, Ar*H*), 7.51–7.62 (m, 8H, Ar*H*), 8.31–8.4 (m, 8H, Ar*H*); ^{13}C NMR ($CDCl_3$) δ 14.1 (CH_3), 21.0 (CH_3), 22.7 (CH_2), 28.5 (CH_2), 30.1 (CH_2), 31.5 (CH_2), 31.8 (CH_2), 58.8 (CH_2), 62.8 (CH_2), 63.0 (CH_2), 102.0 (*C*H), 107.6 (*C*H), 107.7 (*C*H), 124.6 (*C*H), 124.7 (*C*H), 124.8 (*C*H), 125.1 (*C*H), 125.2 (*C*H), 126.1 (*C*H), 126.3 (*C*H), 126.3 (*C*H), 128.6 (*C*), 129.3 (*C*), 129.4 (*C*), 130.3 (*C*H), 130.8 (*C*), 130.9 (*C*), 131.0 (*C*), 138.1 (*C*), 160.5 (*C*), 160.7 (*C*), 171.2 (*C*). Anal. Calcd for $C_{45}H_{42}O_4$: C, 83.56; H, 6.54; N, 0.00. Found: C, 83.49; H, 6.34; N, 0.00.

4.1.10. Synthetic procedure for 15B. A solution containing **14B** (1.07 g, 1.14 mmol) and sodium methoxide (0.20 g, 3.70 mmol) in a mixture of methanol (15 mL) and THF (15 mL) was heated to reflux with stirring under argon atmosphere. After 12 h, the reaction mixture was cooled to room temperature, and concentrated in vacuo. Dissolving the resulting material in chloroform (20 mL), insoluble solid was removed by filtration through Celite. After the solvent was removed in vacuo, the residue was purified by recrystallization from chloroform–hexane solution to give **15B** (0.97 g, 95%) as a pale yellow powder: mp 214–216 °C; IR (KBr) 1597 cm^{-1} (C=C), 3568 cm^{-1} (OH); MS (FAB, positive) *m/z* 893 (*M*+), 894 (*MH*+); ^{1}H NMR ($CDCl_3$) δ 0.92 (t, *J*=7.1 Hz, 6H, $(CH_2)_5CH_3$), 1.32–1.45 (m, 8H, $(CH2)_3(CH_2)_2CH_3$), 1.55–1.62 (m, 4H, $(CH_2)_2CH_2(CH_2)2CH_3$), 1.76–1.85 (m, 4H, $CH_2CH_2(CH_2)_3CH_3$), 3.63 (t, *J*=8.1 Hz, 4H, $CH_2(CH_2)_4CH_3$), 5.68 (br s, 2H, CH_2OH), 5.90 (s, 2H, CH_2), 5.91 (s, 4H, CH_2), 6.66 (d, *J*=2.0 Hz, 2H, Ar*H*), 6.70 (t, *J*=2.0 Hz, 1H, Ar*H*), 7.49–7.61 (m, 12H, Ar*H*), 8.31–8.36 (m, 10H, Ar*H*), 8.46–8.49 (m, 2H, Ar*H*); ^{13}C NMR ($CDCl_3$) δ 14.1 (CH_3), 22.7 (CH_2), 28.5 (CH_2), 30.1 (CH_2), 31.4 (CH_2), 31.8 (CH_2), 57.6 (CH_2), 62.9 (CH_2), 63.1 (CH_2), 94.9 (*C*H), 95.0 (*C*H), 124.6 (*C*H), 124.7 (*C*H), 124.8 (*C*H), 125.1 (*C*H), 125.2 (*C*H), 126.1 (*C*H), 126.2 (*C*H), 126.3 (*C*H), 128.4 (*C*), 129.4 (*C*), 130.1 (*C*), 130.9 (*C*), 131.0 (*C*), 133.3 (*C*), 138.2 (*C*), 161.2 (*C*), 161.4 (*C*). Anal. Calcd for $C_{64}H_{62}O_4$: C, 85.87; H, 6.98; N, 0.00. Found: C, 85.95; H, 7.14; N, 0.00.

4.1.11. Synthetic procedure for 15L. A solution containing **14L** (0.74 g, 1.14 mmol) and sodium methoxide (0.20 g, 3.70 mmol) in a mixture of methanol (20 mL) and THF (25 mL) was heated to reflux with stirring under argon atmosphere. After 12 h, the reaction mixture was cooled to room temperature, and concentrated in vacuo. Dissolving the resulting material in chloroform (20 mL), insoluble solid was removed by filtration through Celite. After the solvent was removed in vacuo, the residue was purified by recrystallization from chloroform–hexane solution to give **15L** (0.64 g, 92%) as a pale yellow powder: mp 207–208 °C; IR (KBr) 1579 cm^{-1} (C=C), 3423 cm^{-1} (C=O); MS (FAB+) *m/z* 604 (*M*+), 605 (*MH*+); ^{1}H NMR ($CDCl_3$) δ 0.92 (t, *J*=6.8 Hz, 3H, $(CH_2)_5CH_3$), 1.30–1.46 (m, 4H, $(CH_2)_3(CH_2)_2CH_3$), 1.57–1.66 (m, 2H, $(CH_2)_2CH_2(CH_2)_2CH_3$), 1.74 (t, *J*=5.4 Hz, 1H, O*H*), 1.80–1.87 (m, 2H, $CH_2CH_2(CH_2)_3CH_3$), 3.64 (t, *J*=8.1 Hz, 2H, $CH_2(CH_2)_4CH_3$), 5.72 (d, *J*=5.4 Hz, 2H, CH_2OH), 5.95 (s, 2H, CH_2), 5.96 (s, 2H, CH_2), 6.85–6.90 (m, 2H, Ar*H*), 6.97 (br s, 1H, Ar*H*), 7.36–7.41 (m, 1H, Ar*H*), 7.49–7.62 (m, 8H, Ar*H*), 8.31–8.37 (m, 6H, Ar*H*), 8.48–8.52 (m, 2H, Ar*H*); ^{13}C NMR ($CDCl_3$) δ 14.1 (CH_3), 22.7 (CH_2), 28.5 (CH_2), 30.1 (CH_2), 31.4 (CH_2), 31.8 (CH_2), 57.6 (CH_2), 62.8 (CH_2), 63.0 (CH_2), 101.9 (*C*H), 107.5 (*C*H), 107.7 (*C*H), 124.6 (*C*H), 124.7 (*C*H), 124.8 (*C*H), 125.1 (*C*H), 125.2 (*C*H), 126.1 (*C*H), 126.2 (*C*H), 126.3 (*C*H), 128.4 (*C*), 129.3 (*C*), 130.0 (*C*), 130.3 (*C*H), 130.9 (*C*), 131.0 (*C*), 133.2 (*C*), 138.1 (*C*), 160.5 (*C*), 160.6 (*C*). Anal. Calcd for $C_{43}H_{40}O_3$: C, 85.40; H, 6.67; N, 0.00. Found: C, 85.10; H, 6.64; N, 0.00.

4.1.12. Synthetic procedure for 7B. To a solution containing **15B** (0.37 g, 0.41 mmol), 4-dimethylaminopyridine (0.10 g, 0.82 mmol), lithium chloride (0.52 g, 12.3 mmol), and triethylamine (1.15 mL, 8.25 mmol) in anhydrous THF (15 mL), a solution of methanesulfonyl chloride (0.16 mL, 2.07 mmol) in anhydrous THF (5 mL) was added dropwise at 0 °C. After stirring at room temperature for additional 12 h, the reaction mixture was quenched by slow addition of HCl (3.0 mol/L, 10 mL), and then extracted twice with chloroform (30 mL). The combined organic layers were washed with water (20 mL) and brine (20 mL), dried over anhydrous Na_2SO_4, filtered, and concentrated in vacuo. Purification of the residue by recrystallization from chloroform–hexane solution gave **7B** (0.33 g, 87%) as a pale yellow powder: mp 223–225 °C; IR (KBr) 1585 cm^{-1} (C=C); MS (FAB, positive) *m/z* 912 (*M*+), 913 (*MH*+); ^{1}H NMR ($CDCl_3$) δ 0.91 (t, *J*=7.1 Hz, 6H, $(CH_2)_5CH_3$), 1.31–1.42 (m, 8H, $(CH2)_3(CH_2)_2CH_3$), 1.54–1.61 (m, 4H, $(CH_2)_2CH_2(CH_2)_2CH_3$), 1.75–1.85 (m, 4H, $CH_2CH_2(CH_2)_3CH_3$), 3.61 (t, *J*=8.1 Hz, 4H, $CH_2(CH_2)_4CH_3$), 5.57 (s, 2H, CH_2Cl), 5.85 (s, 2H, CH_2), 6.88 (s, 4H, CH_2), 6.64 (d, *J*=2.1 Hz, 2H, Ar*H*), 6.68 (t, *J*=2.1 Hz, 1H, Ar*H*), 7.47–7.62 (m, 12H, Ar*H*), 8.30–8.35 (m, 12H, Ar*H*); ^{13}C NMR ($CDCl_3$) δ 14.1 (CH_3), 22.7 (CH_2), 28.5 (CH_2), 30.1 (CH_2), 31.4 (CH_2), 31.8 (CH_2), 38.9 (CH_2), 62.7 (CH_2), 63.0 (CH_2), 94.9 (*C*H), 95.1 (*C*H), 124.1 (*C*H), 124.7 (*C*H), 124.9 (*C*H), 125.1 (*C*H), 125.2 (*C*H), 126.1 (*C*H), 126.4 (*C*H), 126.6 (*C*H), 129.2 (*C*), 129.4 (*C*), 129.7 (*C*), 130.0 (*C*), 130.9 (*C*), 131.0 (*C*), 138.2 (*C*), 161.1 (*C*), 161.4 (*C*). Anal. Calcd for $C_{64}H_{61}ClO_3$: C, 84.14; H, 6.73; N, 0.00. Found: C, 84.37; H, 6.66; N, 0.02.

4.1.13. Synthetic procedure for 7L. To a solution containing **15L** (0.25 g, 0.41 mmol), 4-dimethylaminopyridine (0.10 g, 0.82 mmol), lithium chloride (0.52 g, 12.3 mmol), and triethylamine (1.15 mL, 8.25 mmol) in anhydrous THF (15 mL), a solution of methanesulfonyl chloride (0.16 mL, 2.07 mmol) in anhydrous THF (5 mL) was added dropwise at 0 °C. After stirring at room temperature for additional 12 h, the reaction mixture was quenched by slow addition of HCl (3.0 mol/L, 10 mL), and then extracted twice with chloroform (30 mL). The combined organic layers were washed with water (20 mL) and brine (20 mL), dried over anhydrous Na_2SO_4, filtered, and concentrated in vacuo. Purification of the residue by recrystallization from chloroform–hexane solution gave **7L**

(0.23 g, 91%) as a pale yellow powder: mp 178–180 °C; IR (KBr) 1589 cm^{-1} (C═C); MS (FAB+) *m/z* 622 (*M*+), 623 (*MH*+); ^{1}H NMR ($CDCl_3$) δ 0.92 (t, J=6.9 Hz, 3H, $(CH_2)_5CH_3$), 1.32–1.44 (m, 4H, $(CH_2)_3(CH_2)_2CH_3$), 1.58–1.66 (m, 2H, $(CH_2)_2CH_2(CH_2)_2CH_3$), 1.77–1.85 (m, 2H, $CH_2CH_2(CH_2)_3CH_3$), 3.64 (t, J=8.1 Hz, 2H, $CH_2(CH_2)_4CH_3$), 5.64 (s, 2H, CH_2Cl), 5.95 (s, 4H, CH_2), 6.84–6.98 (m, 2H, Ar*H*), 7.39 (t, J=8.3 Hz, 1H, Ar*H*), 7.50–7.67 (m, 8H, Ar*H*), 8.31–8.40 (m, 8H, Ar*H*); ^{13}C NMR ($CDCl_3$) δ 14.1 (CH_3), 22.7 (CH_2), 28.5 (CH_2), 30.1 (CH_2), 31.5 (CH_2), 31.8 (CH_2), 39.0 (CH_2), 62.7 (CH_2), 63.0 (CH_2), 102.0 (*C*H), 107.6 (*C*H), 107.7 (*C*H), 124.2 (*C*H), 124.7 (*C*H), 125.0 (*C*H), 125.1 (*C*H), 125.2 (*C*H), 126.1 (*C*H), 126.4 (*C*H), 126.6 (*C*H), 129.4 (*C*), 129.8 (*C*), 130.0 (*C*), 130.3 (*C*H), 130.9 (*C*), 131.0 (*C*), 138.2 (*C*), 160.4 (*C*), 160.7 (*C*). Anal. Calcd for $C_{43}H_{39}ClO_2$: C, 82.87; H, 6.31; N, 0.00. Found: C, 82.56; H, 6.17; N, 0.08.

4.1.14. Synthetic procedure for 3B. A solution containing **7B** (0.15 g, 0.16 mmol), **5** (0.018 g, 0.074 mmol), potassium carbonate (0.028 g, 0.20 mmol), and 18-crown-6 (0.039 g, 0.15 mmol) in DMF (5 mL) was heated at 55 °C with stirring under argon atmosphere. After 4 h, the reaction mixture was cooled to room temperature, and poured into saturated ammonium chloride solution to precipitate the product. The precipitate was collected by filtration, intensively washed with water, and dried in a vacuum to afford a pale yellow solid. Purification of the residue by silica-gel column chromatography (80% chloroform, 20% hexane) and recrystallization from chloroform–hexane solution gave **3B** (0.11 g, 75%) as a pale yellow powder: mp 135–137 °C; UV ($CHCl_3$) 358 nm (ε 33,800), 378 nm (ε 54,700), 398 nm (ε 54,100); IR (KBr) 1591 cm^{-1} (C═C), 1720 cm^{-1} (C═O); MS (ESI, positive) *m/z* 2020.9 (*MNa*+), 2036.9 (*MNaO*+), 2052.9 ($MNaO_2$+), 2069.0 ($MNaO_3$+); ^{1}H NMR ($CDCl_3$) δ 0.88 (t, J=7.1 Hz, 12H, $(CH_2)_5CH_3$), 1.25–1.37 (m, 16H, $(CH_2)_3(CH_2)_2CH_3$), 1.48–1.55 (m, 8H, $(CH_2)_2CH_2(CH_2)_2CH_3$), 1.66–1.79 (m, 8H, $CH_2CH_2(CH_2)_3CH_3$), 3.45–3.57 (m, 8H, $CH_2(CH_2)_4CH_3$), 5.28 (s, 2H, CH_2OBz), 5.74 (s, 16H, CH_2O), 6.60 (s, 4H, Ar*H*), 6.62 (s, 2H, Ar*H*), 6.82 (s, 3H, Ar*H*), 7.26–7.35 (m, 3H, Ar*H*), 7.38–7.50 (m, 24H, Ar*H*), 8.02–8.04 (m, 2H, Bz*H*), 8.15–8.27 (m, 24H, Ar*H*); ^{13}C NMR ($CDCl_3$) δ 14.1 (CH_3), 22.7 (CH_2), 28.4 (CH_2), 30.0 (CH_2), 31.4 (CH_2), 31.7 (CH_2), 62.7 (CH_2), 62.9 (CH_2), 66.4 (CH_2), 94.8 (*C*H), 95.0 (*C*H), 101.2 (*C*H), 107.3 (*C*H), 124.7 (*C*H), 125.0 (*C*H), 125.1 (*C*H), 126.0 (*C*H), 126.2 (*C*H), 128.3 (*C*H), 128.8 (*C*), 129.0 (*C*), 129.3 (*C*), 129.7 (*C*H), 130.0 (*C*), 130.6 (*C*), 130.7 (*C*), 130.9 (*C*), 133.0 (*C*H), 138.0 (*C*), 138.8 (*C*), 160.6 (*C*), 161.2 (*C*), 161.3 (*C*), 166.3 (*C*). Anal. Calcd for $C_{142}H_{132}O_{10}$: C, 85.34; H, 6.66; N, 0.00. Found: C, 85.28; H, 6.63; N, 0.00.

4.1.15. Synthetic procedure for 3L. A solution containing **7L** (0.12 g, 0.19 mmol), **5** (0.022 g, 0.090 mmol), potassium carbonate (0.034 g, 0.25 mmol), and 18-crown-6 (0.047 g, 0.18 mmol) in DMF (5 mL) was heated at 55 °C with stirring under argon atmosphere. After 4 h, the reaction mixture was cooled to room temperature, and poured into saturated ammonium chloride solution to precipitate the product. The precipitate was collected by filtration, intensively washed with water, and dried in a vacuum to afford a pale yellow solid. Purification of the residue by silica-gel column chromatography (80% chloroform, 20% hexane) and recrystallization from chloroform–hexane solution gave **3L** (0.088 g, 69%) as a pale yellow powder: mp 141–142 °C; UV ($CHCl_3$) 357 nm (ε 23,400), 375 nm (ε 37,400), 396 nm (ε 37,000); IR (KBr) 1589 cm^{-1} (C═C), 1718 cm^{-1} (C═O); MS (ESI, positive) *m/z* 1471.5 ($MNaO_2$+); ^{1}H NMR ($CDCl_3$) δ 0.92 (t, J=6.6 Hz, 6H, $(CH_2)_5CH_3$), 1.26–1.44 (m, 8H, $(CH_2)_3(CH_2)_2CH_3$), 1.51–1.62 (m, 4H, $(CH_2)_2CH_2(CH_2)_2CH_3$), 1.73–1.87 (m, 4H, $CH_2CH_2(CH_2)_3CH_3$), 3.58–3.64 (m, 4H, $CH_2(CH_2)_4CH_3$), 5.39 (s, 2H, CH_2OBz), 5.91 (s, 4H, CH_2O), 5.93 (s, 4H, CH_2O), 5.95 (s, 4H, CH_2O), 6.82–6.95 (m, 9H, Ar*H*), 7.33–7.42 (m, 5H, Ar*H*), 7.49–7.55 (m, 16H, Ar*H*), 8.08–8.11 (m, 2H, Bz*H*), 8.26–8.36 (m, 16H, Ar*H*); ^{13}C NMR ($CDCl_3$) δ 14.1 (CH_3), 22.7 (CH_2), 28.5 (CH_2), 30.1 (CH_2), 31.4 (CH_2), 31.8 (CH_2), 62.9 (CH_2), 63.0 (CH_2), 66.5 (CH_2), 101.4 (*C*H), 102.0 (*C*H), 107.3 (*C*H), 107.6 (*C*H), 107.8 (*C*H), 124.7 (*C*H), 125.0 (*C*H), 125.2 (*C*H), 126.0 (*C*H), 126.3 (*C*H), 129.3 (*C*H), 128.4 (*C*), 128.9 (*C*), 129.2 (*C*), 129.8 (*C*), 130.2 (*C*), 130.8 (*C*H), 130.9 (*C*), 138.1 (*C*), 160.5 (*C*), 160.6 (*C*), 166.4 (*C*). Anal. Calcd for $C_{100}H_{88}O_8$: C, 84.72; H, 6.26; N, 0.00. Found: C, 84.74; H, 6.28; N, 0.00.

4.1.16. Synthetic procedure for 4B. A solution containing **7B** (0.55 g, 0.61 mmol), **6** (0.043 g, 0.075 mmol), potassium carbonate (0.094 g, 0.68 mmol), and 18-crown-6 (0.18 g, 0.68 mmol) in DMF (10 mL) was heated at 55 °C with stirring under argon atmosphere. After 4 h, the reaction mixture was cooled to room temperature, and poured into saturated ammonium chloride solution to precipitate the product. The precipitate was collected by filtration, intensively washed with water, and dried in a vacuum to afford a yellow solid. Purification of the residue by the preparative HPLC (chloroform as eluent) gave **4B** (0.25 g, 57%) as a yellow powder: mp 136–137 °C; UV ($CHCl_3$) 359 nm (ε 106,000), 378 nm (ε 171,000), 399 nm (ε 167,000); IR (KBr) 1593 cm^{-1} (C═C), 1728 cm^{-1} (C═O); MS (CSI, negative) *m/z* 2954.5 ($MCl_2$2−), 5873.3 (*MCl*−); ^{1}H NMR ($CDCl_3$) δ 0.88 (t, J=6.9 Hz, 36H, $(CH_2)_5CH_3$), 1.28–1.37 (m, 48H, $(CH_2)_3(CH_2)_2CH_3$), 1.52–1.62 (m, 24H, $(CH_2)_2CH_2(CH_2)_2CH_3$), 1.71–1.83 (m, 24H, $CH_2CH_2(CH_2)_3CH_3$), 3.53–3.60 (m, 24H, $CH_2(CH_2)_4CH_3$), 5.31 (s, 6H, CH_2OBz), 5.62 (s, 12H, OCH_2), 5.66 (s, 12H, OCH_2), 5.74 (s, 24H, OCH_2), 6.55 (s, 12H, Ar*H*), 6.61 (s, 6H, Ar*H*), 6.72 (s, 3H, Ar*H*), 6.80 (s, 6H, Ar*H*), 7.37–7.56 (m, 72H, Ar*H*), 8.14–8.35 (m, 72H, Ar*H*), 8.95 (s, 3H, Bz*H*); ^{13}C NMR ($CDCl_3$) δ 14.1 (CH_3), 22.7 (CH_2), 28.4 (CH_2), 30.0 (CH_2), 31.4 (CH_2), 31.7 (CH_2), 62.6 (CH_2), 62.9 (CH_2), 67.1 (CH_2), 94.8 (*C*H), 95.1 (*C*H), 102.1 (*C*H), 107.8 (*C*H), 124.7 (*C*H), 125.0 (*C*H), 125.1 (*C*H), 126.0 (*C*H), 126.1 (*C*H), 128.7 (*C*), 128.9 (*C*), 129.3 (*C*), 130.6 (*C*), 130.9 (*C*), 134.9 (*C*), 138.0 (*C*), 138.1 (*C*), 160.5 (*C*), 161.2 (*C*), 161.3 (*C*), 164.6 (*C*). Anal. Calcd for $C_{414}H_{384}O_{30}$: C, 85.15; H, 6.63; N, 0.00. Found: C, 84.95; H, 6.43; N, 0.00.

4.1.17. Synthetic procedure for 4L. A solution containing **7L** (0.50 g, 0.80 mmol), **6** (0.058 g, 0.10 mmol), potassium carbonate (0.13 g, 0.91 mmol), and 18-crown-6 (0.24 g, 0.91 mmol) in DMF (10 mL) was heated at 55 °C with stirring under argon atmosphere. After 4 h, the reaction mixture was cooled to room temperature, and poured into saturated ammonium chloride solution to precipitate the product. The precipitate was collected by filtration,

intensively washed with water, and dried in a vacuum to afford a yellow solid. Purification of the residue by recrystallization from chloroform solution gave **4L** (0.20 g, 48%) as a pale yellow powder. This compound was so insoluble in $CDCl_3$ and other deuterated solvents that the ^{13}C NMR spectrum could not be recorded: mp 159–160 °C; UV ($CHCl_3$) 358 nm (ε 74,400), 377 nm (ε 113,000), 397 nm (ε 112,000); IR (KBr) 1591 cm^{-1} (C═C), 1726 cm^{-1} (C═O); MS (CSI, negative) *m*/*z* 4131.8 (*MCl*−); ^1H NMR ($CDCl_3$) δ 0.88 (t, $J=6.9$ Hz, 18H, $(CH_2)_5CH_3$), 1.21–1.39 (m, 24H, $(CH_2)_3(CH_2)_2CH_3$), 1.46–1.57 (m, 12H, $(CH_2)_2CH_2(CH_2)_2CH_3$), 1.68–1.82 (m, 12H, $CH_2CH_2(CH_2)_3CH_3$), 3.55–3.62 (m, 12H, $CH_2(CH_2)_4CH_3$), 5.40 (s, 6H, CH_2OBz), 5.73–5.91 (m, 36H, OCH_2), 6.75–6.89 (m, 27H, Ar*H*), 7.24–7.59 (m, 54H, Ar*H*), 8.17–8.31 (m, 48H, Ar*H*), 9.01 (s, 3H, Bz*H*). Anal. Calcd for $C_{288}H_{252}O_{24}$: C, 84.43; H, 6.20; N, 0.00. Found: C, 84.57; H, 6.27; N, 0.16.

Acknowledgements

This research was supported by a Grant-in-Aid for Scientific Research from the Ministry of Education, Culture, Sports, Science, and Technology, Japan (Grant 13740393) and Suzuki Foundation. We thank Dr. Shuichi Hiraoka of the University of Tokyo, Japan for the ESI-MS measurements.

References and notes

1. Tomalia, D. A. *Nature* **1994**, *372*, 617–618.
2. Fréchet, J. M. J. *Science* **1994**, *263*, 1710–1715.
3. Newkome, G. R.; Moorefield, C. N.; Vögtle, F. *Dendritic Molecules Concepts, Synthesis, Perspectives*; VCH: Weinheim, New York, Basel, Cambridge, Tokyo, 1996.
4. Matthews, O. A.; Shipway, A. N.; Stoddart, J. F. *Prog. Polym. Sci.* **1998**, *23*, 1–56.
5. Séverac, M.; Leclaire, J.; Sutra, P.; Caminade, A.-M.; Majoral, J.-P. *Tetrahedron Lett.* **2004**, *45*, 3019–3022.
6. Takahashi, M.; Odagi, T.; Tomita, H.; Oshikawa, T.; Yamashita, M. *Tetrahedron Lett.* **2003**, *44*, 2455–2458.
7. Takahashi, M.; Morimoto, H.; Suzuki, Y.; Odagi, T.; Yamashita, M.; Kawai, H. *Tetrahedron* **2004**, *60*, 11771–11781.
8. Balzani, V.; Ceroni, P.; Gestermann, S.; Kauffmann, C.; Gorka, M.; Vögtle, F. *Chem. Commun.* **2000**, 853–854.
9. Yeow, E. K. L.; Ghiggino, K. P.; Reek, J. N. H.; Crossley, M. J.; Bosman, A. W.; Schenning, A. P. H. J.; Meijer, E. W. *J. Phys. Chem. B* **2000**, *104*, 2596–2606.
10. Choi, M.-S.; Yamazaki, T.; Yamazaki, I.; Aida, T. *Angew. Chem., Int. Ed.* **2003**, *43*, 150–158.
11. Hofkens, J.; Cotlet, M.; Vosch, T.; Tinnefeld, P.; Weston, K. D.; Ego, C.; Grimsdale, A.; Mullen, K.; Beljonne, D.; Bredas, J. L.; Jordens, S.; Schweitzer, G.; Markus, S.; De Schryver, F. *Proc. Natl. Acad. Sci. U.S.A.* **2003**, *100*, 13146–13151.
12. As for an example of dendrimers incorporating anthracene groups at site-specific positions, see: Sivanandan, K.; Aathimanikandan, S. V.; Arges, C. G.; Bardeen, C. J.; Thayumanavan, S. *J. Am. Chem. Soc.* **2005**, *127*, 2020–2021.
13. Huang, R. L.; Williams, P. *J. Chem. Soc.* **1958**, 2637–2640.
14. Zaugg, H. E. *J. Org. Chem.* **1976**, *41*, 3419–3421.
15. Bell, K. H. *Tetrahedron Lett.* **1986**, *27*, 2263–2264.
16. The ESI-MS measurements were conducted in the presence of excess sodium iodide in chloroform–methanol solutions, which led to the observations of sodium adduct ion peaks in a positive ion mode.
17. The CSI-MS measurements were conducted in dichloromethane solutions, which exhibited the chloride adduct ion peaks in a negative ion mode.
18. In view of broad shoulders at longer wavelength ($\lambda_{em}>$ 500 nm) in the fluorescence spectra of **4B** and **4L**, possibilities of intramolecular excimer formations cannot be strictly ruled out.
19. As for detailed mechanistic investigations of energy migration in bisanthracene systems, see: Johansson, L.B.-Å.; Bergström, F.; Edman, P.; Grechishnikova, I. V.; Molotkovsky, J. G. *J. Chem. Soc., Faraday Trans.* **1996**, *92*, 1563–1567.
20. Turro, N. J. *Modern Molecular Photochemistry*; University Science Books: Sausalito, 1991.
21. As for detailed mechanistic investigations of energy transfer in cofacial bisporphyrin systems, see: Faure, S.; Stern, C.; Guilard, R.; Harvey, P. D. *J. Am. Chem. Soc.* **2004**, *126*, 1253–1261.
22. Reproducible experimental results were obtained from the time-resolved fluorescence measurements of the three samples operated under anaerobic and aerobic conditions. This indicates the anthracene groups incorporated within the dendritic architectures were tolerant of oxidative degradation on the time scale of the decay runs.
23. To understand a general trend in changes in fluorescence decay profiles for the branching series of dendritic architectures, the dynamic process of **3B** was also examined by the time-resolved techniques under the same conditions employed for the other cases. As a result, **3B** was found to exhibit anomalous behavior in the fluorescence intensity traces decaying much faster than those of the other samples examined, which was quite difficult to be rationalized on the basis of the interpretations stated above. Details on these experimental results will be discussed elsewhere.
24. Nagvekar, D. S.; Gibson, H. W. *Org. Prep. Proced. Int.* **1997**, *29*, 240–242.